JJMIE

Volume 16, Number 3, June. 2022
ISSN 1995-6665
Pages 449 – 458

Jordan Journal of Mechanical and Industrial Engineering

Performance analysis of solar absorption ice maker driven by parabolic trough collector

Mohamad H. Okour*[1], Hamza Al-Tahaineh[1], Wael Al-Kouz[2]

[1] *Mechanical Engineering Department - Al-Huson University College - Al-Balqa Applied University - P. O. Box 50, AlHuson 19117, Irbid, Jordan*

[2] *College of Engineering and Technology, American University of the Middle East, Kuwait*

Received 28 Dec 2021 *Accepted 2 Apr 2022*

Abstract

The current research investigates the use of a two-stage ammonia-water double lift absorption cycle for residential house cooling. The main idea is to store the ice that is produced during the day so that it can be used to cool the building at night when the sun is not available. The Engineering Equation Solver (EES) program was used to simulate and investigate the relationships between different parameters in this cycle. The initial conditions such as the mass fraction difference between weak and strong solution, Mass fraction of ammonia in the evaporator, the temperature of the evaporator, and the ambient temperature.

The result showed that The heat transfer rate in absorber2 is 128.3 kW, the heat transfer rate in desorber2 is 195.4 kW, and the Evaporator heat transfer rate is 23.8 kW, indicating that 350 kg of ice is required to meet the cooling needs of the house at evaporator temperature 223 K and a COP of 0. 1216.

Keywords: Adsorption system, Solar ice makers, COP, EES program.

Nomenclature

Notation	Description	unit
$\dot{m}$	Mass flow rate	(Kg/s)
h	Specific enthalpy	(Kj/Kg)
S	Specific entropy	(Kj/Kg-K)
Q	Quality	(Kg vapor/Kg)
X	Mass fraction of ammonia	(Kgammonia/Kg)
$\dot{Q}$	Rate of heat transfer	(Kw)
$\dot{W}$	Mechanical power	(Kw)
COP	Coefficient of performance	
Cp	Specific heat capacity	(Kj/Kg-K)
E	Energy	(Kj)
η	Efficiency	
ε	Effectiveness	
G	Global radiation	(Kw/m2)
N	Number of solar collectors	
DX	mass fraction difference between weak and strong solution	(Kgammonia/Kg)

1. Introduction

Throughout the history of humankind, major advances in civilization have been accompanied by increased consumption of energy, which seems to be a major factor in the industrial power available and in the level of living of individuals. The existence of vast supplies of energy mostly leads to high rates of industrial growth. Furthermore, the availability of a low-cost energy source might lead to inefficient utilization of energy.

The world's hunger for energy has grown dramatically in the last few centuries, thus new sources of energy must be found and more efficient methods of utilizing them for different applications must be developed.

Fossil fuels, such as coal, gas, and oil, are the most common nonrenewable energy sources. These natural resources are a major source of energy for a wide range of industries; however, non-renewable energy has several drawbacks, including a negative environmental impact and a limited supply. Renewable energy, also known as clean energy, is derived from natural sources or processes that are replenished regularly. Sunlight and wind, for example, continue to shine and blow even though their availability is dependent on time and weather.

Solar energy could be utilized either by converting it to heat or to electricity, both of these forms have numerous applications like heating, cooling, food drying, and many more.

Sun's heat can be utilized to create cold by the usage of solar thermal cooling technologies like absorption and adsorption cycles.

In general, the ice demand increases for many fields requiring ice like food service, hospitals, industries,

* Corresponding author e-mail: okour123@bau.edu.jo.

restaurants, hotels, laboratories, sports arenas, air conditioning, and various other places where large quantities of ice are needed continuously with different shapes and sizes. this incremental demand on ice makes it an attractive field for investment.

The requirement of a system that is fast and economically justified is necessary. Ice is used in this wide range of applications because it is safe for health, cheap handling equipment for chemical and physical properties, available everywhere and does not have bad side effects on foods or drinks.

A thermally driven adsorption chiller, integrated in a cooling tower, is used in the sun cooling project (water cooled system). Evacuated tube collectors provide heat to the chiller. Flat plate solar collectors were employed to deliver heat to the System of Solar Adsorption Refrigeration because the adsorption chillers demand a lower supply temperature to the generator, which can be easily produced by flat panel solar collectors [1].

For the use of medium-temperature solar energy, an adsorption ice maker with an energy storage system is proposed. The solar energy collected by the parabolic trough collector (PTC) was used to heat the adsorption ice maker in this system. The icemaker's performance was evaluated, and the highest coefficient of performance (COP) was found to be 0.15 experimentally [2].

The presented work investigates the use of a commercial freezer to efficiently produce ice using photovoltaic energy. The compressor's operation is adapted to the availability of solar energy using an innovative control unit. The proposed solar ice-maker was investigated using simulations and experiments. A design methodology for optimizing the solar energy supply system for a target ice production of 12 kilograms per day[3].

It was proposed to use a distributed photovoltaic energy system (DPES) to power an ice storage air conditioning system (ISACS). In addition, the optimization of system structure was investigated. The theoretical calculations and experimental tests were analyzed by the energy coupling and transferring characteristics in the light-electricity-cold conversion process. The system's energy utilization efficiency was found to be 4.64 percent [4].

An experiment using a working pair of activated carbon (AquaSorb 2000) and methanol for a solar adsorption ice maker system (SAIMS) [5].

1.1. The single-stage solar absorption cycle

A solar collector or concentrator, a hot fluid storage tank, an auxiliary heater, condenser, evaporator, expansion device, and thermal compressor make up a typical solar absorption cooling system. A generator, an absorber, and a mixture circulating pump, as well as a pressure reducing device (expansion device), make up the thermal compressor. The solution pump uses a small amount of energy compared to the mechanical compressor.

Absorption occurs when a substance in one state interpenetrates and combines with another substance in a different state. The two phases have a strong affinity for exothermically forming a solution or a mixture. This process can be reversed by heating the mixture and releasing the absorbed phase from the absorbent.

To power these systems, most absorption cooling systems use a single-stage absorption cycle with an H2O/LiBr working pair and either a solar flat plate collector or an evacuated tube collector with hot water. As shown in Figure 1, the single-stage solar absorption cooling system is based on the Basic absorption cycle, which has a single absorber and generator. The heat provided by the solar collector separates the refrigerant from the absorbent in the generator. The vapor-refrigerant condenses in the condenser, then expands in expansion valve 1, and evaporates in the evaporator at low pressure and temperature. A weak solution returns from the generator after passing through the expansion valve 2 and absorbs the cold refrigerant in the absorber. The rich mixture created in the absorber is pumped back to the generator by the pump. To improve the cycle efficiency, a typical solution heat exchanger can be used. The absorber is chilled by cooling water because the absorption is exothermic.

The aim of this study is to demonstrate that the two-stage ammonia-water double lift absorption cycle used in the solar absorption ice maker is thermally driven. Since absorption chillers based on double effect technology have the potential to convert solar energy more effectively while utilizing less primary energy produced by parabolic trough collectors. The Engineering Equation Solver (EES) program was used to simulate and investigate the relationships between different parameters in the cycle that was carried out for this purpose. The objective of our work is to conduct a thermal investigation of an ammonia-water two-stage double lift absorption cycle for solar ice makers and its application in air conditioning applications.

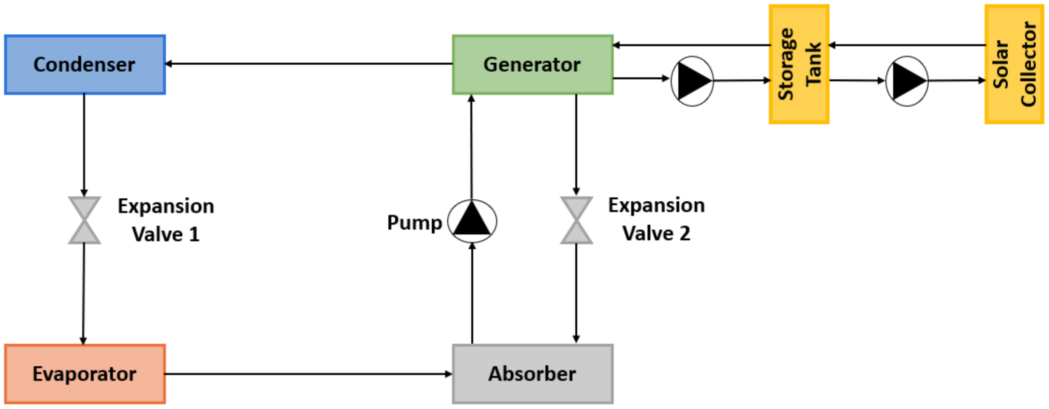

Figure 1. Single-effect solar absorption cycle

2. System Description:

2.1. Two-stage Solar Absorption Cycle

A double effect system can be achieved by adding an extra stage to the single effect cycle as a topping cycle. Absorption chillers based on the double effect technology have potential to convert solar energy more effectively while using less primary energy. They have a nearly double COP value when compared to single-effect systems (COP = 1.2). Their working liquids, on the other hand, must reach higher temperatures, exceeding 130ºC, which is outside the range for which most solar collectors are designed.

As shown in Figure (2), this absorption cycle, like water/LiBr two-stage cycles, uses the heat of the condenser to run desorber 1, and the flow in the intermediate solution circuit is reversed, reversing the function of these two component, as well as the pump and expansion valve.

The first law of thermodynamics is used to do an energy analysis. Where the first law of thermodynamics for an open system, or any component in an open system, is written as:

$$\left.\frac{dE}{dt}\right|_{cv} = \dot{Q} - \dot{W}_{cv} + \dot{m}_i\left(h_i + \frac{1}{2}V_i^2 + gz_i\right) - \dot{m}_o\left(h_o + \frac{1}{2}V_o^2 + gz_o\right) \quad (1)$$

Each system component can be modeled as a control volume with inlet and outlet streams, heat transfer from or to the system, and/or work done on or by the system. Each component is taken as a single unit, the mass, and energy balance equations for the generator (G), condenser (C), evaporator (E), absorber (A), and auxiliary equipment like solution heat exchanger (SHX), rectifier (rec), and condensate precooler (Cprecooler) are established.

$$\sum \dot{m}_{in} - \sum \dot{m}_{out} = 0 \quad (2)$$

$$\dot{Q} = \sum \dot{m}_{out} h_{out} - \sum \dot{m}_{in} h_{in} = 0 \quad (3)$$

The COP of the system is an indication of how efficient the cooling or heating process is, the COP of any cooling cycle is given by equation (4).

$$COP_{actual} = \frac{Q_E}{Q_{Des2} + W_{pump1} + W_{pump2}} \quad (4)$$

However, because Q_E and Q_{Des2} is too much larger than W_{pump1} and W_{pump2} so, the actual COP is given by:

$$COP_{actual} = \frac{Q_E}{Q_{Des2}} \quad (5)$$

The actual COP of the refrigeration cycle should be compared to the Carnot COP (Maximum possible COP).

2.2. Ice calculation

A house in Amman Jordan was used to test the affordability of this method of cooling. The load of the house shown in figure (13), was calculated and the solar irradiation at the same place was calculated using PHOTOVOLTAIC GEOGRAPHICAL INFORMATION SYSTEM, then available Q_{evap} was calculated by the following equation:

$$Q_{evaporator} = \eta_{collecter}\, N\, A_{collecter}\, G\, COP \quad (6)$$

Where:

$Q_{evaporator}$: rate of heat absorbed by the evaporator (KW)

$\eta_{collecter}$: collector efficiency

N: number of collectors.

$A_{collector}$: the area of the collector (m^2)

G: global radiation (KW/m^2)

COP: coefficient of performance for the absorption cycle.

Figure (3), depicts the distribution of solar irradiation at Amman, Jordan during the day, with radiation values for beam, diffuse, and global radiation.

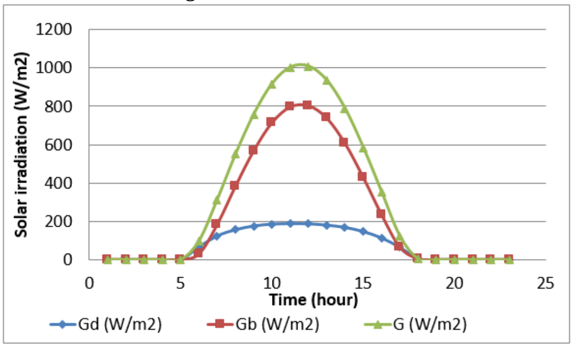

Figure 3. the hourly distribution of solar irradiation in Amman Jordan

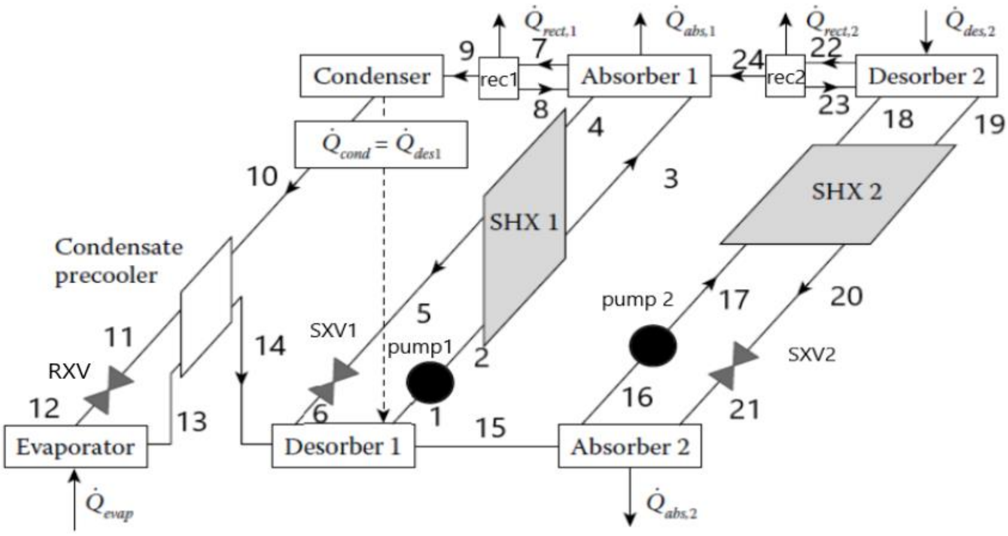

Figure 2. Two-stage double lift absorption refrigeration cycle

A parabolic trough collector is used in this simulation because of its relatively high efficiency, collector efficiency of 0.75, and collector Aperture area of 4 m^2 were assumed.

Next, an equation of conservation of energy is established to determine the energy available in the stored ice at any given time in the day given the $Q_{evaporator}$, Ql_{oad}, and the amount of energy already stored in the ice.

$$E_{gen} + E_{in} - E_{out} = \Delta E_{system} \quad (7)$$

Where:

E_{gen}: the energy generated inside the system (the system is considered to be the ice tank) (Kj)

E_{in}: the energy entering the system (Kj)

E_{out}: the energy leaving the system (Kj)

ΔE_{system}: the energy accumulation inside the system. (Kj)

differentiating equation (7) with respect to time leads to:

$$\dot{Q}_{gen} + \dot{Q}_{in} - \dot{Q}_{out} = \dot{Q}_{system} \quad (8)$$

Where:

$\dot{Q}_{gen}$: energy generation rate (KW)

$\dot{Q}_{in}$: the rate of energy entering the system (KW), in this case, it is Q_{load}

$\dot{Q}_{out}$: the rate of energy leaving the system (KW), in this case, it is $Q_{evaporator}$

$\dot{Q}_{system}$: energy accumulation rate inside the system (KW).

The following is the relationship between the amount of energy in the system and the rate of heat accumulation:

$$E_{system} = \int \dot{Q}_{system}\, dt + E_0 \quad (9)$$

This can be written as considering $\dot{Q}_{gen}$ is none existed:

$$E_{system} = \int (\dot{Q}_{load} - \dot{Q}_{evaporator})\, dt + E_0 \quad (10)$$

Where:

E_{system}: the energy stored in ice (Kj) at a given time.

E_0: energy the ice possesses initially (Kj); at hour zero.

The model was built on EES, it was assumed that the cycle's COP is 0.1216 at evaporator temperature of 223 K, it was found that using this model, the number of solar collectors needed to cover building's cooling loads for the entire day was found to be 60, Figure (4) represents the energy stored in the ice throughout the day.

By knowing the maximum energy stored in ice (minimum energy value) and the minimum temperature, the mass of ice can be calculated by using equation (11) as follows:

$$M_{ice} = \frac{E_{system\ min}}{h_{ice}} \quad (11)$$

Where:

M_{ice}: mass of stored ice (Kg)

$E_{system\ min}$: minimum energy stored in ice along the day (Kj)

h_{ice}: specific enthalpy of ice (Kj/Kg)

The mass of ice was found to be 352 Kg using equation (11). Ice temperature throughout the day can now be found as in Figure (5).

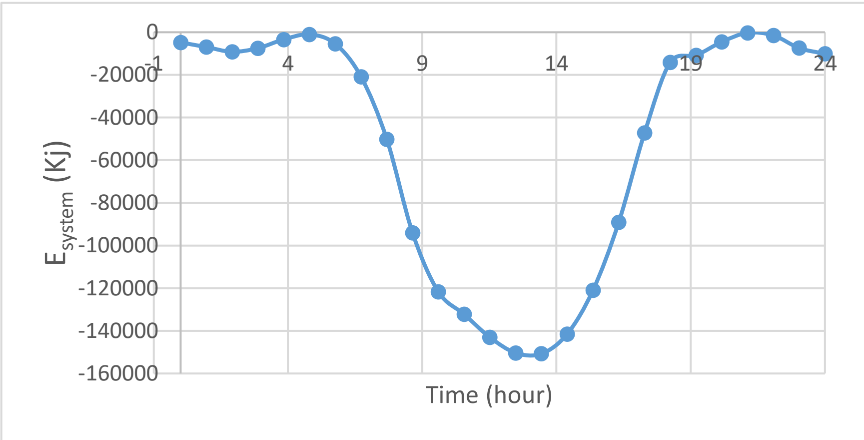

Figure 4. energy stored in ice throughout the day

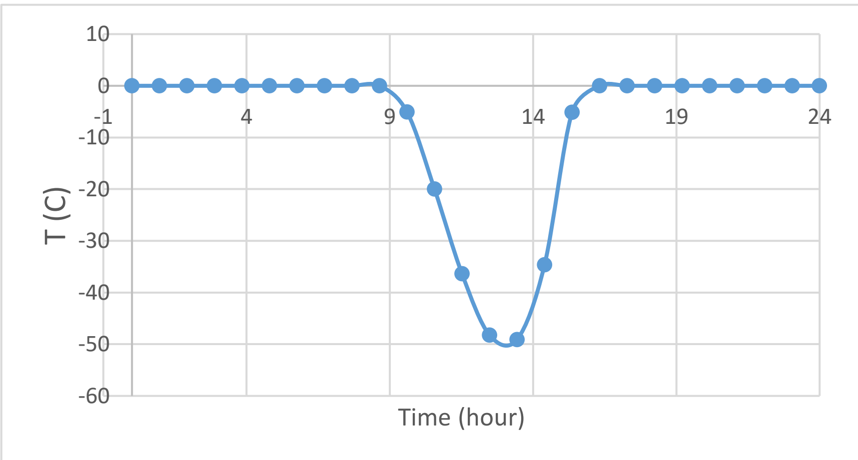

Figure 5. Ice temperature profile along the day

An overview of the ice maker used to make and store ice (and water) is made, the device should be able to store all the needed ice with acceptable heat transfer rates to both the ice and air, the device should also be able to transfer sensible heat only in which the humidity ration does not change along with it as shown in figure (6).

3. Results and Analysis

The simulation results are shown and discussed. For this aim, some parameters (Evaporator's Outlet Temperature, Evaporators Exit Quality, Refrigerant mass fraction, mass fraction difference between weak and strong solution (DX), Ambient Temperature) were compared. Furthermore, a comparison between this cycle and the single-stage ammonia-water cycle was done.

Figure (7) shows the relation between the COP and evaporator's exit quality, the COP increases

to a certain point as the evaporator's exit quality increases, then falls as the evaporator's exit quality increases, the model can simulate for evaporator's exit quality values less than 0.98, however, a drop in COP occurs at high-quality values (higher than 0.93). This is due to the dramatic drop in pressure of the refrigerant at such high-quality values as in Figure (8), this drop in pressure causes the COP to drop as explained previously.

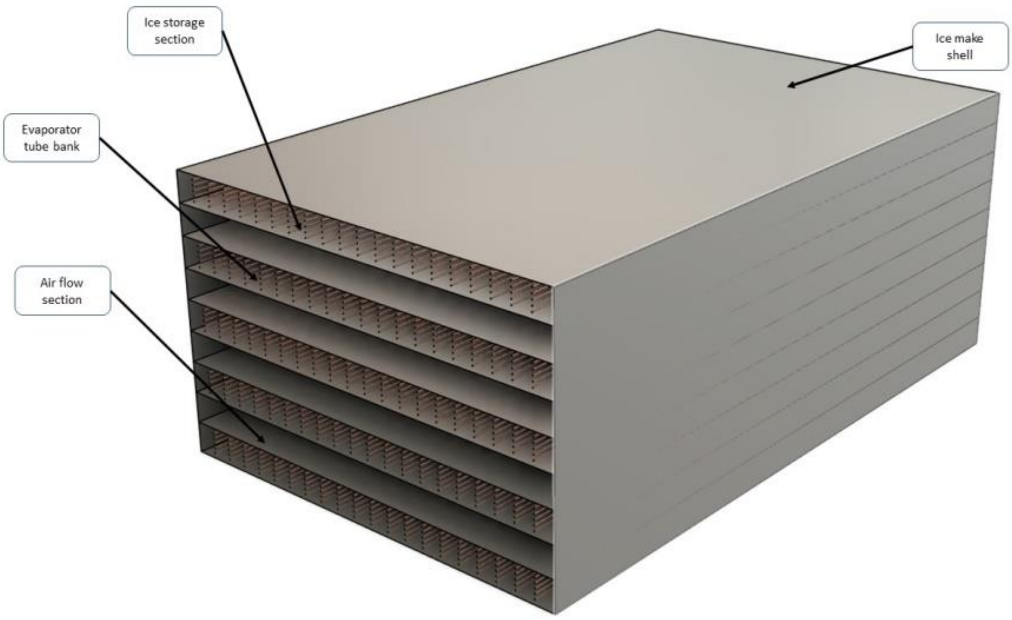

Figure 6. view of an ice maker

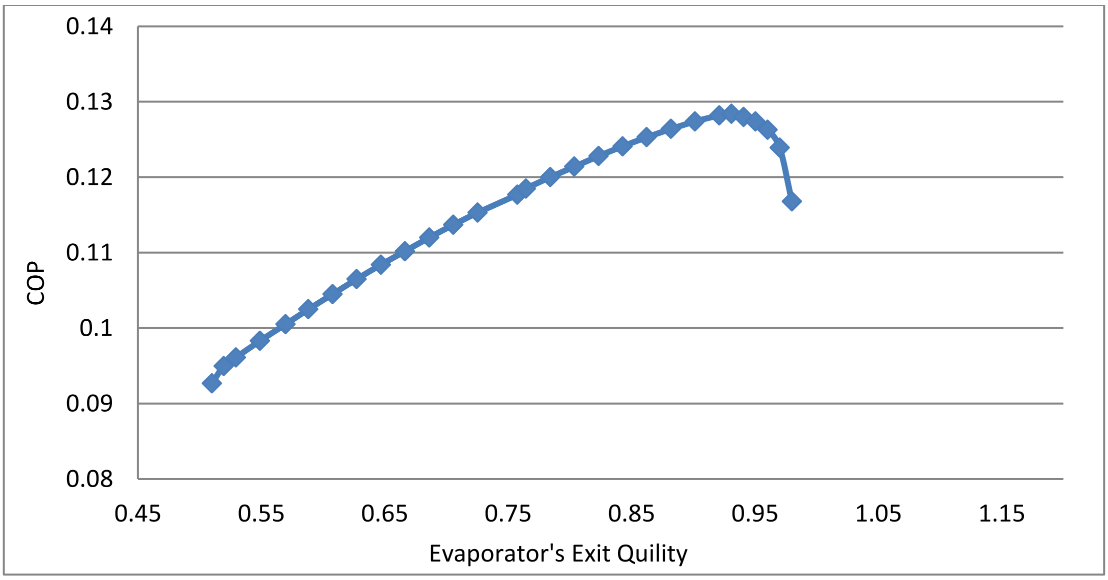

Figure 7. COP relation to evaporators exit quality

Figure (9) shows the relation between the COP against refrigerant mass fraction, as expected; the COP increases as the refrigerant mass fraction increases due to the pressure increase, higher pressure leads to lower heat capacity at the desorber2 outlets, consequently to lower desorber2 heat. The simulation model is valid for values of refrigerant mass fraction lower than 0.9907.

Figure (10) illustrates the relationship between the COP and the mass fraction difference in the solution circuits (DX), the model can simulate DX values between 0.02 and 0.115, the results show that the COP is directly related to the DX value due to the decrease of the energy required at the desorber 2, however, this is due to the decrease in the mass fraction of point 19 (the weak solution line) which results in a decrease in the mass flow rates at points 18 (the strong solution line) and 19 while keeping the mass flow rates at point 22 (vapor line) and 23 (condensate line from rectifier) nearly constant.

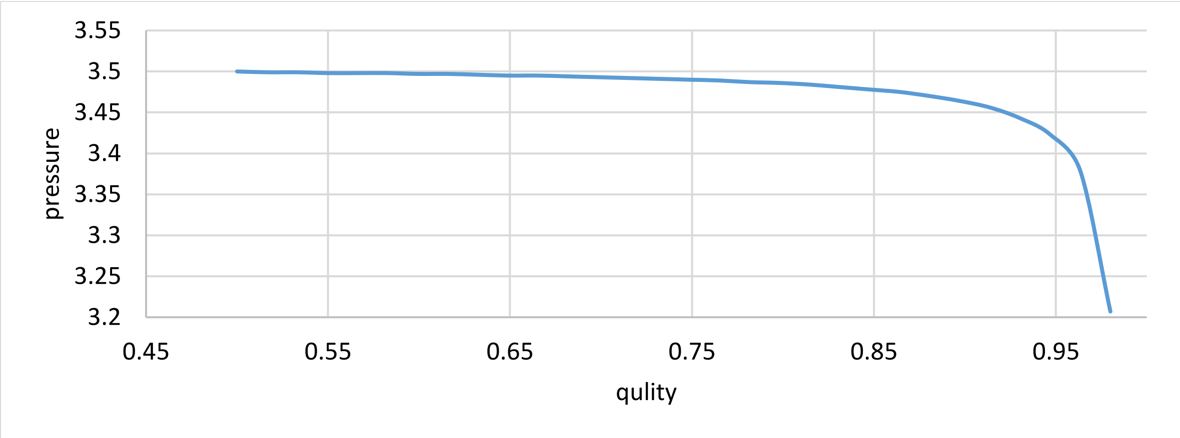

Figure 8. pressure and quality relationship of the ammonia-water mixture at a constant concentration

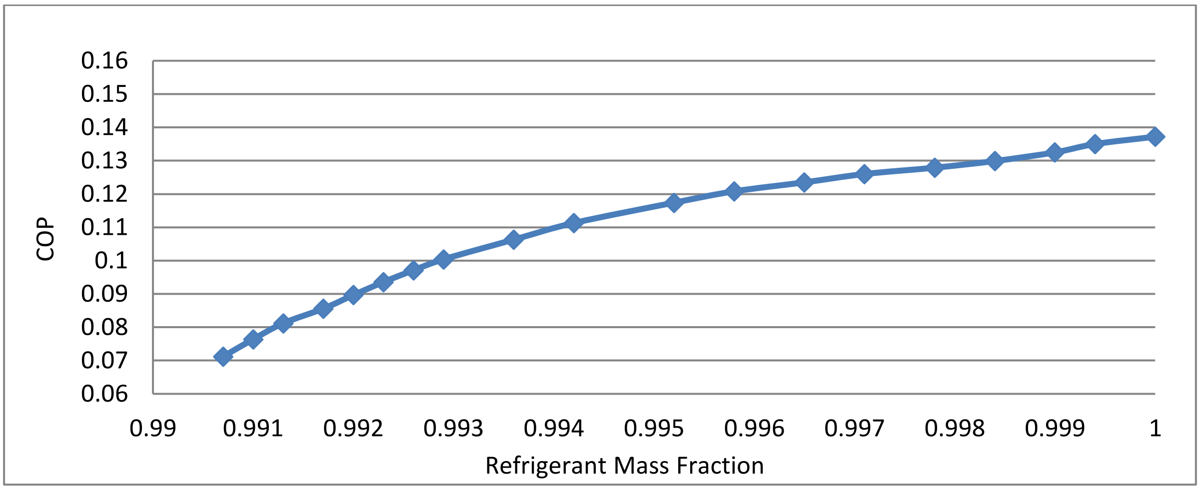

Figure 9. COP relation to Refrigerant mass fraction

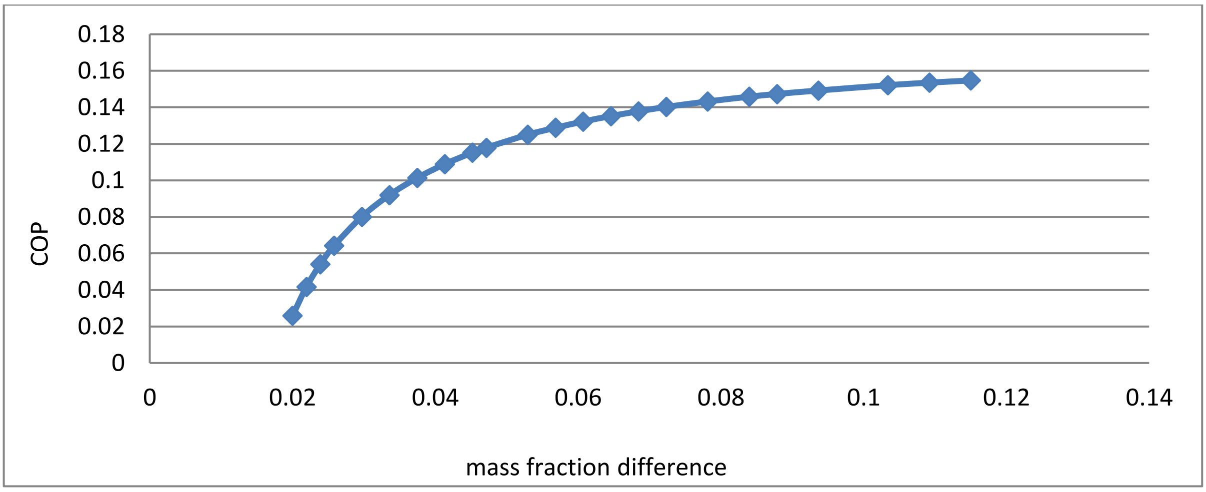

Figure 10. COP relation to mass fraction difference in the solution circuits

Figure (11) demonstrates that the higher the ambient temperature the lower the COP. This is mainly due to lower values of ammonia concentrations at the weak and strong solution lines at the desorber 2 which in turn results in an increase in the mass flow rates at these lines, thus increasing the desorber2 required heat. This result also follows the Carnot law of maximum efficiency.

A comparison between a single-stage ammonia absorption cycle and the two-stage double lift cycle is shown in Figure (12). despite the single-stage cycle has a higher COP value, it runs on a smaller range of evaporator temperatures and with a higher desorber temperature than the two-stage double lift cycle. The simulated data for the cycle illustrated in Figure 2 is provided in Tables 1 and 2.

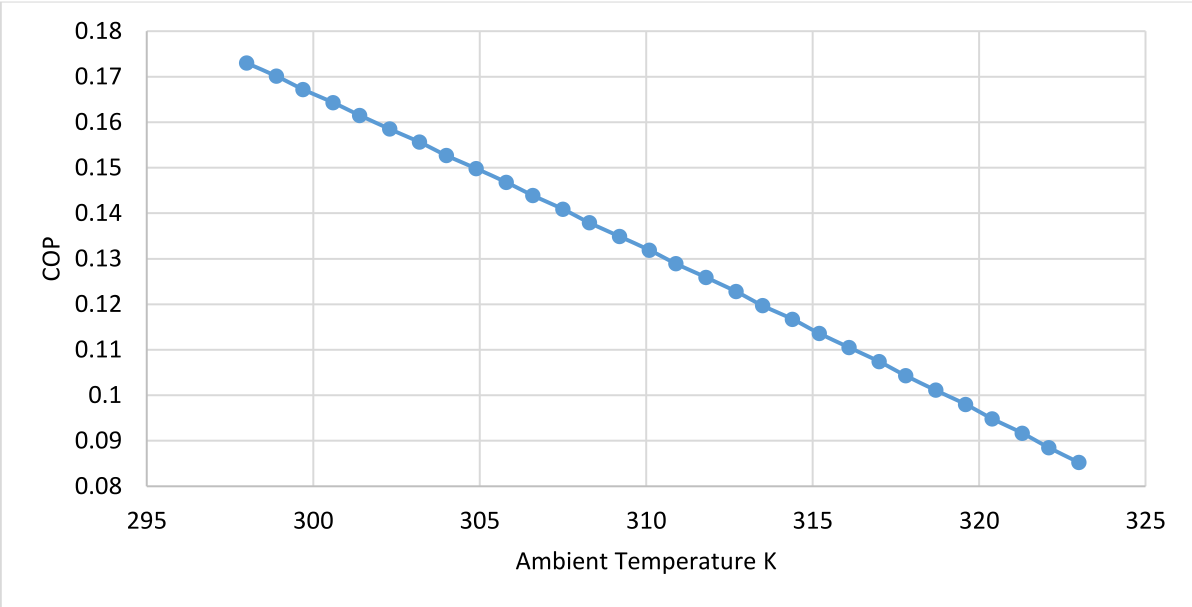

Figure 11. COP relation to Ambient Temperature

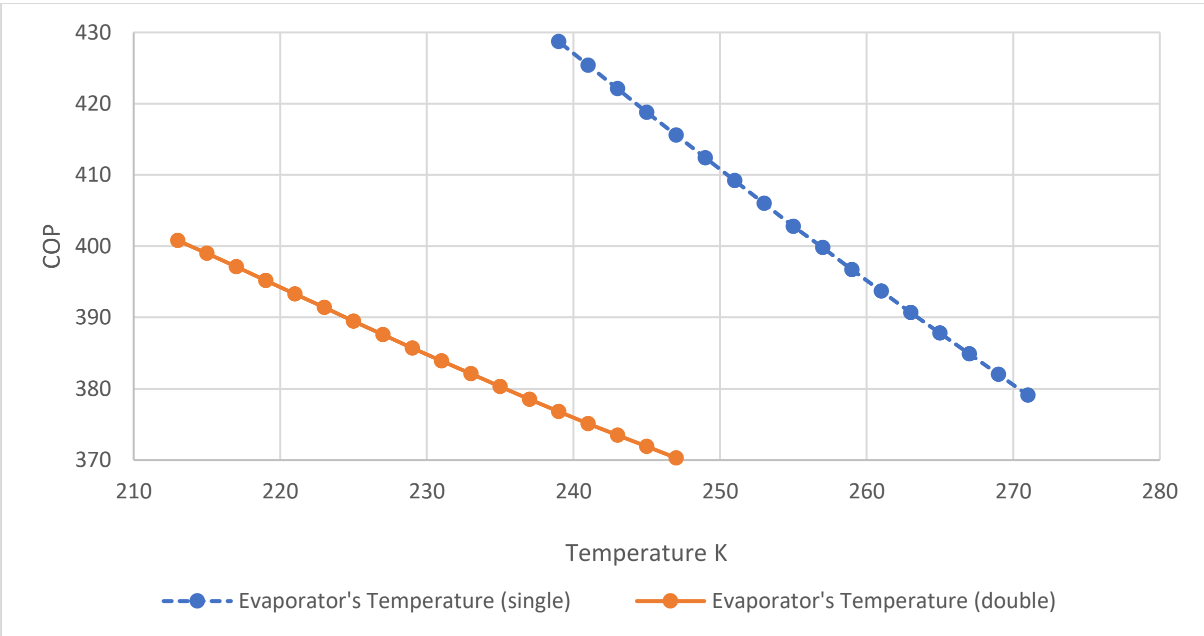

Figure 12. A comparison between single-stage and two-stage double lift cycles with respect to evaporator and desorber operating temperatures.

Table 1. simulated data for the cycle

State Points	m (kg/sec)	P (bar)	T (°C)	h (KJ/Kg)	x (kg/kg)	Vapor Quality
1	0.2849	0.3428	266.4	-250.1	0.3708	0
2	0.2849	3.296	266.4	-249.7	0.3708	-0.001
3	0.2849	3.296	303.6	-85.01	0.3708	-0.001
4	0.3097	3.296	313	-55.14	0.4208	0
5	0.3097	3.296	278.9	-206.7	0.4208	-0.001
6	0.3097	0.3428	262.7	-206.7	0.4208	0.04326
7	0.01846	3.296	313	1382	0.9908	1
8	0.000166	3.296	313	-55.36	0.4208	0
9	0.01829	3.296	303	1352	0.996	1.001
10	0.01829	3.296	266.4	-33.96	0.996	0
11	0.01829	3.296	242.4	-141.8	0.996	-0.001
12	0.01829	0.3428	220.3	-141.8	0.996	0.06907
13	0.01829	0.3428	223	1159	0.996	0.975
14	0.01829	0.3428	258	1267	0.996	0.9958
15	0.04309	0.3428	266.4	1294	0.9956	1
16	0.8025	0.3428	313	89.88	0.1144	0
17	0.8025	3.296	313	90.19	0.1144	-0.001
18	0.8025	3.296	372.4	340.3	0.1144	-0.001
19	0.7594	3.296	391.4	454.7	0.06444	0
20	0.7594	3.296	328.8	190.4	0.06444	-0.001
21	0.7594	0.3428	325.8	190.4	0.06444	0.006265
22	0.06964	3.296	378.2	1908	0.6597	1
23	0.02655	3.296	378.2	366.2	0.1144	0
24	0.04309	3.296	304.4	1353	0.9956	1

Table 2. simulated data for the cycle

Summary of Energy Quantities		
$\dot{w}p_1$	Pump1 power	0.09556kW
$\dot{w}p_2$	Pump2 power	0.2503kW
$\dot{Q}_{SHX1}$	Heat transfer rate in solution SHX1	46.93kW
$\dot{Q}_{SHX2}$	Heat transfer rate in solution SHX2	200.7kW
$\dot{Q}_{precooler}$	Heat transfer rate in precooler	1.973kW
$\dot{Q}_{abs1}$	Heat transfer rate in absorber1	25.64kW
$\dot{Q}_{abs2}$	Heat transfer rate in absorber2	128.3kW
$\dot{Q}_{rect1}$	Heat transfer rate in rectifier1	0.7754kW
$\dot{Q}_{rect2}$	Heat transfer rate in rectifier2	64.87kW
$\dot{Q}_{des1}$	Heat transfer rate in desorber1	25.36kW
$\dot{Q}_{des2}$	Heat transfer rate in desorber2	195.4kW
$\dot{Q}_{cond}$	Condenser heat transfer rate	25.36kW
$\dot{Q}_{evap}$	Evaporator heat transfer rate	23.8kW
COP	Cycle coefficient of performance	0.1216

4. Discreet method

The available data of solar radiation is hourly based, thus the evaporator's capacity can be determined for each hour using eq. (6), Figure (13) shows the evaporator's capacity as well as building load along the day.

By using Microsoft Excel sheet, the data for the evaporator's capacity and building load were implemented, the hourly difference between both of these values was found as (ΔQ), where:

$$\Delta Q = \dot{Q}_{load} - \dot{Q}_{evap} \quad (12)$$

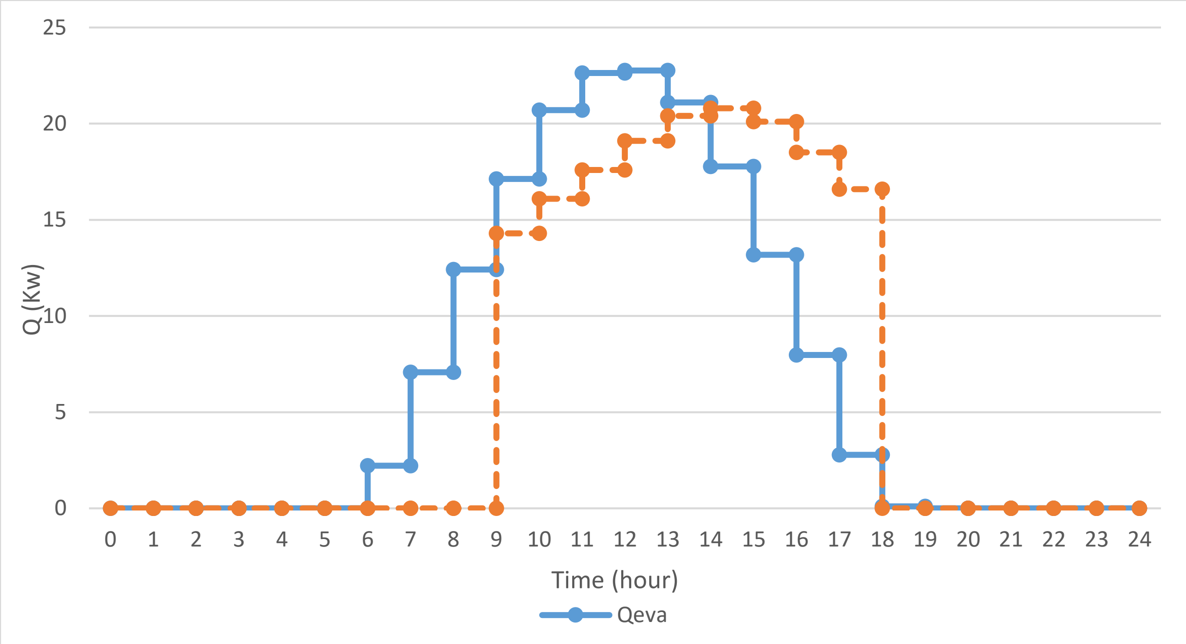

Figure 13. hourly evaporator's capacity and building load throughout the day.

Using this method, The number of solar collectors was found to be 61 and the mass of ice needed is found to be 350 Kg.

5. conclusions

The two-stage double lift ammonia-water absorption cycle model is limited by some of its parameters, going outside the limits would result in negative mass flow rates or unsatisfactory saturation properties.

This cycle operates at lower operating temperatures than the single-stage cycle, on the other hand, it has lower COP. Changing the cycle with one with higher COP while using the same evaporator design and ice storage principle might be more profitable.

This cycle can benefit from other sources of heat other than solar, it can be driven by a steam turbine condenser waste heat or geothermal heat since it runs on low generation temperatures.

The results obtained by the continuous method are very close to the results obtained using the discreet method. The result showed that the mass of ice needed to cover the house cooling needs is approximately 350 Kg at evaporator temperature of 223 K with a Cycle coefficient of performance COP of about 0.1216, while the Heat transfer rate in absorber2 is 128.3 kW, the Heat transfer rate in desorber2 is 195.4 kW, the Condenser heat transfer rate is 25.36 kW and the Evaporator heat transfer rate is 23.8 kW.

References

[1] Al-Rbaihat R. ‹Sakhrieh A., Al-Asfar J., Alahmer A., Ayadi O, Al-Salaymeh A., Al_hamamre Z., Al- bawwab A., Hamdan M., Performance Assessment and Theoretical Simulation of Adsorption Refrigeration System Driven by Flat Plate Solar Collector. Jordan Journal of Mechanical and Industrial Engineering JJmie,Vol. 11 (1), 2017, 1-11.

[2] Li, C., et al., Experimental study on an adsorption icemaker driven by parabolic trough solar collector. Renewable Energy, 57: p. 223-233,2013.

[3] Torres-Toledo, V., et al., Design and performance of a small-scale solar ice-maker based on a DC-freezer and an adaptive control unit. Solar Energy, 139: p. 433-443, 2016.

[4] Xu, Y., et al., Performance analysis of ice storage air conditioning system driven by distributed photovoltaic energy. Bulg Chem Commun, 48: p. 165-172, 2016.

[5] Attalla, M., et al., Experimental study of solar-powered ice maker using adsorption pair of activated carbon and methanol. Applied Thermal Engineering, 141: p. 877-886, 2018.

[6] Bataineh K. M., Gharaibeh A., Optimization Analyses of Parabolic Trough (CSP) Plants for the Desert Regions of the Middle East and North Africa (MENA). Jordan Journal of Mechanical and Industrial Engineering JJmie,Vol. 12 (1), 2018, 33-43.

[7] Ababneh A., Energy Conservation Using a Double-effect Absorption Cycle Driven by Solar Energy and Fossil Fuel. Jordan Journal of Mechanical and Industrial Engineering JJmie,Vol. 5 (3), 2011, 213-219.

[8] Moreno-Quintanar, G., W. Rivera, and R. Best. Development of a solar intermittent refrigeration system for ice production. in World Renewable Energy Congress-Sweden; 8-13 May; 2011; Linköping; Sweden. 2011. Linköping University Electronic Press.

[9] EESI Environmental and Energy Study Institute. 13/3/2020. Fossil Fuels. https://www.eesi.org/topics/fossilfuels/description?fbclid=IwAR0JcW2Iv3YrwCY4usR64FWHX52FXCm40aP4asBzXNfuVd6EPR5ch5-OayA

[10] Besagni, G., R. Mereu, and F. Inzoli, Ejector refrigeration: a comprehensive review. Renewable and Sustainable Energy Reviews, 53: p. 373-407, 2016.

[11] Zhang, X. and R. Wang, A new combined adsorption–ejector refrigeration and heating hybrid system powered by solar energy. Applied Thermal Engineering, 22(11): p. 1245-1258, 2002.

[12] Reddy, P.J.P. and S.S. Murthy, Studies on an Ejector-Absorption Refrigeration Cycle with New Working Fluid Pairs.

[13]Energy Developments: New Forms, Renewables, Conservation. Solar Furnace, 1984.

]14] Hamza Abdel-Latif Al-Tahaineh. Second Law Analysis of Solar Powered Absorption Refrigeration System, 2002.

[15] Photovoltaic geographical information system. 15/10/2019. Position information and standard conditions.

[16]Keith E.Herold Reinhard Radermacher Sanford A.Klein. Absorption Chillers and Heat Pumps. 2nd ed, 2016.

[17] Petros J. Axaopoulos, Michael P. Theodoridis, Design and experimental performance of a PV Ice-maker without battery. Solar Energy, 83(8):1360-1369, August 2009.

[18] Bu, X.B., Li, H.S., Wang, L.B., Performance analysis and working fluids selection of solar powered organic rankine-vapor compression ice maker. Sol. Energy 95, 271–278, 2013.

[19] M. Navidbakhsh, Ali Shirazi, S. Sanaye, Four E analysis and multi-objective optimization of an ice storage system incorporating PCM as the partial cold storage for air-conditioning applications. Applied Thermal Engineering, Volume 58, Issues 1–2, Pages 30-41, 2013.

[20] M. Rosen, I. Dincer, Norman Pedinelli, Thermodynamic Performance of Ice Thermal Energy Storage Systems. Journal of Energy Resources Technology-transactions of The Asme, 122(4): 205-211 (7 pages), 2000.

[21] Beggs, C., The Economics of Ice Thermal Storage. Building Research and Information, 19 , No. 6 , pp. 342 – 355, 1991.

[22] Michel Pons , J. J. Guilleminot , Design of an Experimental Solar-Powered, Solid-Adsorption Ice Maker. Journal of Solar Energy Engineering, 108(4): 332-337, 1986.

[23] Z. F. Li And K. Sumathy, A Solar-Powered Ice-Maker with the Solid Adsorption Pair of Activated Carbon and Methanol. International Journal of Energy Research, 23, 517— 527, 1999.